ADV MATH SCI JOURNAL
Advances in Mathematics: Scientific Journal **10** (2021), no.9, 3273–3282
ISSN: 1857-8365 (printed); 1857-8438 (electronic)
https://doi.org/10.37418/amsj.10.9.16

THREE-DIMENSIONAL STAGNATION-POINT FLOW OVER A PERMEABLE STRETCHING/SHRINKING SHEET WITH A SECOND ORDER SLIP FLOW

Mohd Ezad Hafidz Hafidzuddin[1], Roslinda Nazar, Norihan M. Arifin, and Ioan Pop

ABSTRACT. The problem of steady laminar three-dimensional stagnation-point flow on a permeable stretching/shrinking sheet with second order slip flow model is studied numerically. Similarity transformation has been used to reduce the governing system of nonlinear partial differential equations into the system of ordinary (similarity) differential equations. The transformed equations are then solved numerically using the `bvp4c` function in MATLAB. Multiple solutions are found for a certain range of the governing parameters. The effects of the governing parameters on the skin friction coefficients and the velocity profiles are presented and discussed. It is found that the second order slip flow model is necessary to predict the flow characteristics accurately.

1. INTRODUCTION

The study of stagnation point-flows is important due to its numerous applications in industry, such as flows over the tips of aircrafts and submarines. Hiemenz [1] was the first to obtain an exact solution for the two-dimensional stagnation-point flow against a stationary semi-infinite wall. Later, Hiemenz's

[1]*corresponding author*

2020 *Mathematics Subject Classification.* 34B15, 65L10, 76-10, 76D05.
Key words and phrases. Stagnation point flow, Three dimensional, Stretching/shrinking sheet, Second order slip, Dual solution.
Submitted: 23.07.2021; *Accepted:* 26.08.2021; *Published:* 30.09.2021.

work was extended by Homann [2] to the axisymmetric case. Libby [3] extended Homann's work to the case of three-dimensional stagnation flow towards a moving plate. The flows induced by a plate moving normal to planar (Hiemenz) and axisymmetric (Homann) stagnation-point flows was discussed by Weidman and Sprague [4]. Very recently, Khashi'ie et al. [5] investigated the effect of suction on the stagnation point flow of hybrid nanofluid toward a permeable and vertical Riga plate.

In 2008, Wu [6] proposed a second order slip flow model for rarefied gas flows at arbitrary Knudsen number, which is based on numerical simulation of linearized Boltzmann equation. Following [6], Fang et al. [7] studied the viscous flow over a shrinking sheet, while Nandeppanavar et al. [8] discussed the second order slip flow and heat transfer over a stretching sheet with non-linear Navier boundary condition. Soid et al. [9] studied the axisymmetric stagnation-point flow over a stretching/shrinking vertical surface with a second-order velocity slip and temperature jump. Recently, Waini et al. [10] examined the behaviour of a hybrid nanofluid flow towards a stagnation point on a stretching or shrinking surface with second-order slip and melting heat transfer effects.

To date, it is seen in the literature that a proper numerical study of second order slip flow for a three dimensional stagnation-point flow is scarce. Therefore, the main purpose of this paper is to extend the work in [9] by considering the three-dimensional stagnation-point flow. The governing partial differential equations are first transformed into a system of ordinary differential equations, and then solved numerically by using the `bvp4c` function.

2. Mathematical Formulation

Consider the steady three-dimensional laminar boundary layer stagnation-point flow of a viscous fluid past a permeable stretching/shrinking sheet. The Cartesian coordinates x, y and z are measured in the $xy-$plane, while fluid is placed along the $z-$axis. We assume that the constant mass flux velocity is denoted by w_0, where $w_0 < 0$ is for suction and $w_0 > 0$ is for injection. Under these assumptions, the governing boundary layer equations can be written as

$$\frac{\partial u}{\partial x} + \frac{\partial v}{\partial y} + \frac{\partial w}{\partial z} = 0, \tag{2.1}$$

$$u\frac{\partial u}{\partial x}+v\frac{\partial u}{\partial y}+w\frac{\partial u}{\partial z}=u_e\frac{du_e}{dx}+\nu\frac{\partial^2 u}{\partial z^2}, \tag{2.2}$$

$$u\frac{\partial v}{\partial x}+v\frac{\partial v}{\partial y}+w\frac{\partial v}{\partial z}=v_e\frac{dv_e}{dy}+\nu\frac{\partial^2 v}{\partial z^2}, \tag{2.3}$$

$$u\frac{\partial w}{\partial x}+v\frac{\partial w}{\partial y}+w\frac{\partial w}{\partial z}=w_e\frac{dw_e}{dz}+\nu\frac{\partial^2 w}{\partial z^2}, \tag{2.4}$$

where u, v and w are the velocities along x, y and z directions, respectively, $u_e(x)=ax$, $v_e(x)=ay$ and $w_e(z)=-2az$ are the velocities of the outer (inviscid) flow, and is the kinematic viscosity of the fluid. The boundary conditions are given as

$$\begin{aligned}&u=u_w(x)=\lambda U_w(x)+u_{sl}(x),\ v=v_w(y)=\lambda V_w(y)+v_{sl}(y),\ w=w_0 \text{ at } z=0,\\ &u\to u_e(x),\ v\to v_e(y),\ w\to w_e(z) \text{ as } z\to\infty.\end{aligned} \tag{2.5}$$

where λ is the stretching ($\lambda>0$) or shrinking ($\lambda<0$) parameter. Here, we assume that $U_w(x)=ax$ and $V_w(x)=ay$, where a is a positive constant. Further, u_{sl} and v_{sl} are the slip velocities at the sheet along the x and y direction, respectively, as given by Wu [6]. In this paper, we extend the slip velocities to a three-dimensional slip flow, as following [9]:

$$\begin{aligned}u_{sl}(x)&=\frac{2}{3}\left(\frac{3-\varphi l^3}{\varphi}-\frac{3}{2}\frac{1-l^2}{K_n}\right)\vartheta\frac{\partial u}{\partial z}-\frac{1}{4}\left(l^4+\frac{2}{K_n^2}\left(1-l^2\right)\right)\vartheta^2\frac{\partial^2 u}{\partial z^2},\\ &=A_x\frac{\partial u}{\partial z}+B_x\frac{\partial^2 u}{\partial z^2},\end{aligned} \tag{2.6}$$

$$\begin{aligned}v_{sl}(y)&=\frac{2}{3}\left(\frac{3-\varphi l^3}{\varphi}-\frac{3}{2}\frac{1-l^2}{K_n}\right)\vartheta\frac{\partial v}{\partial z}-\frac{1}{4}\left(l^4+\frac{2}{K_n^2}\left(1-l^2\right)\right)\vartheta^2\frac{\partial^2 v}{\partial z^2},\\ &=A_y\frac{\partial v}{\partial z}+B_y\frac{\partial^2 v}{\partial z^2},\end{aligned} \tag{2.7}$$

where $\varphi(0\le\varphi\le1)$ is the momentum accommodation coefficient, A_x, B_x, A_y and B_y are constants, K_n is a Knudsen number, l is defined as $l=\min(1/K_n,1)$, and $\vartheta(>0)$ is the molecular mean free path. Based on the definitions of l and ϑ, for any number of K_n, it results in that A_x and A_y are always positive, while B_x and B_y are always negative. The subscripts x and y denote the slip velocities for x and $y-$axis, respectively.

We now introduce the following similarity variables

$$u = axf'(\eta),\ v = ayg'(\eta),\ w = \sqrt{a\nu}\left(f(\eta) + g(\eta)\right),\ \eta = z\sqrt{a/\nu}, \tag{2.8}$$

where primes denote the differentiation with respect to η. Here, $s = -w_0/\sqrt{a\nu}$ is defined as surface mass transfer with $s < 0$ for injection and $s > 0$ for suction, respectively, which then gives $f(0) + g(0) = s$. Without loss of generality to the velocity, we can write $f(0) = s,\ g(0) = 0$. Substituting (2.8) into equations (2.1)-(2.4), equation (2.1) is automatically satisfied, while equations (2.2) and (2.3) are reduced to the following ordinary differential equations

$$f''' + (f + g)\,f'' - f'^2 + 1 = 0, \tag{2.9}$$

$$g''' + (f + g)\,g'' - g'^2 + 1 = 0, \tag{2.10}$$

and the boundary conditions (2.5) become

$$\begin{aligned} &f(0) = s,\ g(0) = 0,\\ &f'(0) = \lambda + a_1 f''(0) + b_1 f'''(0),\\ &g'(0) = \lambda + a_2 g''(0) + b_2 g'''(0),\\ &f'(\eta) \to 1,\ g'(\eta) \to 1 \text{ as } \eta \to \infty, \end{aligned} \tag{2.11}$$

where a_1 and a_2 $(a_1, a_2 > 0)$ are the first order slip velocity parameters, while b_1 and b_2 $(b_1, b_2 < 0)$ are the second order slip velocity parameters, which are defined as $a_1 = A_x\sqrt{\frac{a}{\nu}},\ a_2 = A_y\sqrt{\frac{a}{\nu}},\ b_1 = B_x\frac{a}{\nu},\ b_2 = B_y\frac{a}{\nu}$.

The quantities of physical interest are the local skin friction coefficients C_{fx} and C_{fy}, which are given as

$$C_{fx} = \frac{\nu}{U_w^2}\left(\frac{\partial u}{\partial z}\right)_{z=0},\ C_{fy} = \frac{\nu}{V_w^2}\left(\frac{\partial v}{\partial z}\right)_{z=0}. \tag{2.12}$$

Substituting (2.8) into (2.12), we obtain the following

$$Re_x^{1/2} C_{fx} = f''(0),\ Re_y^{1/2} C_{fy} = g''(0), \tag{2.13}$$

where $Re_x = U_w x/\nu$ and $Re_y = V_w y/\nu$ are the local Reynolds numbers based on $U_w(x)$ and $V_w(y)$, respectively.

3. Results and Discussion

Numerical solutions to the governing nonlinear ordinary differential equations (2.9) and (2.10) subject to the boundary conditions (2.11) were obtained using the `bvp4c` function in Matlab for some values of the governing parameters. To verify the accuracy of the present method, a comparison for the values of the reduced skin friction coefficients $f''(0)$ has been made with those of [9]. The comparisons, as shown in Table 1, are found to be in excellent agreement, and thus we are confident that the present method is accurate.

TABLE 1. Comparison values of $f''(0)$ when $\lambda = 0$, $s = 0$, $a_2, b_1, b_2 = 0$.

a_1	[9]	Present study
0	1.311938	1.311938
1	0.617300	0.617300
5	0.179287	0.179284
10	0.094597	0.094597

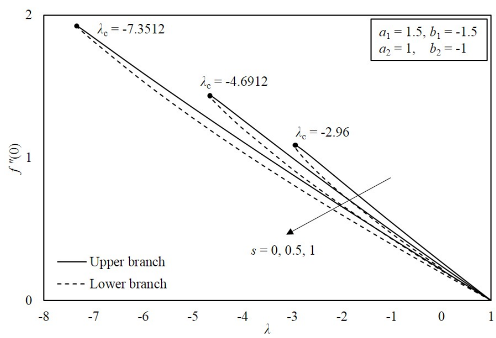

FIGURE 1. Variations of $f''(0)$ with λ for different values of s

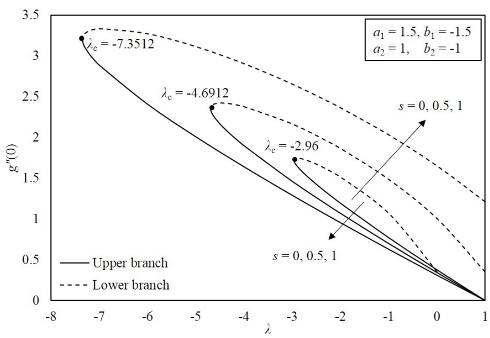

FIGURE 2. Variations of $g''(0)$ with λ for different values of s

Variations of $f''(0)$ and $g''(0)$ with λ for different values of s are presented in Figs. 1 and 2. Dual (upper and lower branch) solutions are found in these figures. The upper and lower branch solutions are illustrated with solid and dashed lines, respectively. It seems that there is no solution for $s < s_c$, where s_c is the critical values of s. Beyond these critical values, the boundary layer separates from the surface and thus the solution based upon the boundary layer approximations are not possible. From the figures, it can be seen that the values of $f''(0)$ and $g''(0)$ increase with the increase of s, while opposite behavior is observed for the lower branch solution $g''(0)$. In addition, $f''(0)$ and $g''(0)$ are seen to decrease to negative when the sheet is stretching ($\lambda > 0$).

Figs. 3 and 4 display the variations of $f''(0)$ and $g''(0)$ with λ for different values of first order slip parameters a_1, a_2 when $s = 2$ and $b_1, b_2 = 0$, while Figs. 5 and 6 display the variations of $f''(0)$ and $g''(0)$ with λ for different values of second order slip parameters b_1, b_2 when $s = 2$ and $a_1, a_2 = 0$. The figures show that the values of $f''(0)$ and $g''(0)$ decrease with the increase of the slip parameters a_1, a_2 and b_1, b_2. Increasing slip at the boundary decreases the wall

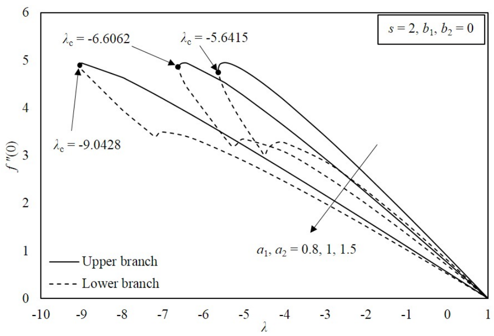

FIGURE 3. Variations of $f''(0)$ with λ for different values of a_1, a_2

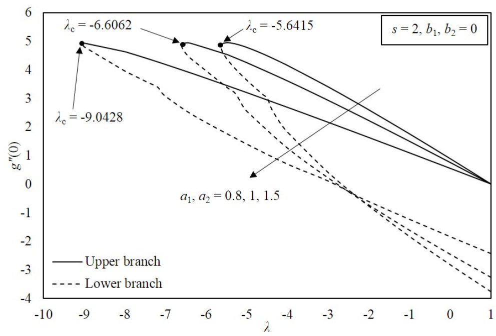

FIGURE 4. Variations of $g''(0)$ with λ for different values of a_1, a_2

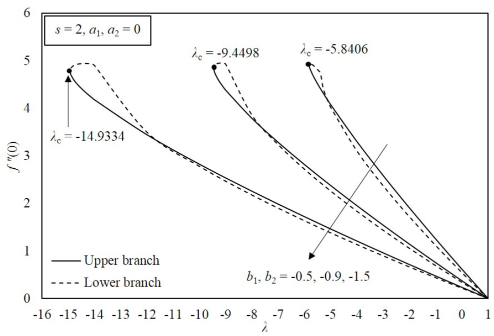

FIGURE 5. Variations of $f''(0)$ with λ for different values b_1, b_2

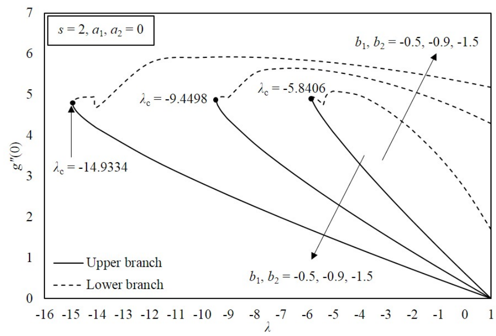

FIGURE 6. Variations of $g''(0)$ with λ for different values b_1, b_2

shear stress, thus reducing the vorticity generated for shrinking velocity due to the weakening fluid adhesion strength. However with the effects of suction, the vorticity remained confined within the boundary layer for larger shrinking velocity, and the steady solution is possible for some large values of λ. Furthermore, this shows that the inclusion of the slip parameters can greatly change the wall drag force [7].

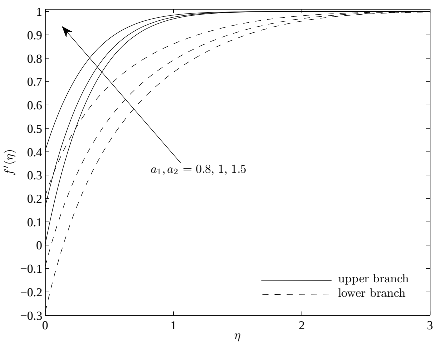

FIGURE 7. Velocity profiles $f'(\eta)$ for different values of a_1 and a_2

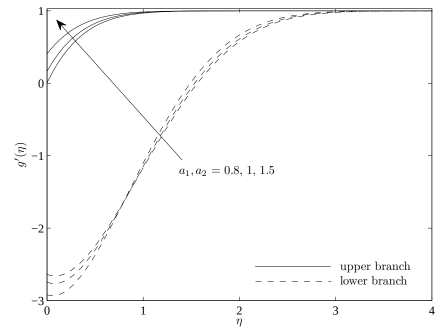

FIGURE 8. Velocity profiles $g'(\eta)$ for different values of a_1 and a_2

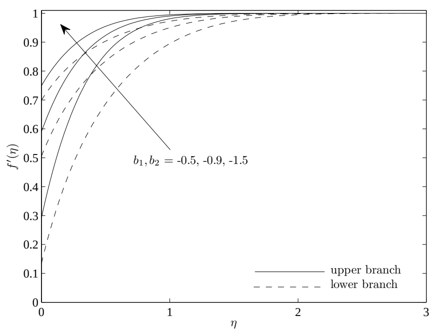

FIGURE 9. Velocity profiles $f'(\eta)$ for different values of b_1 and b_2 when $s = 2$, $\lambda = -2.2$, $a_1, a_2 = 0$

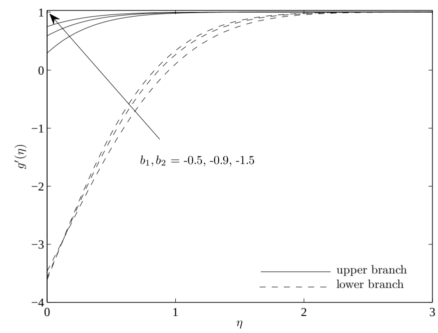

FIGURE 10. Velocity profiles $g'(\eta)$ for different values of b_1 and b_2 when $s = 2$, $\lambda = -2.2$, $a_1, a_2 = 0$

Figs. 7 and 8 illustrate the velocity profiles $f'(\eta)$ and $g'(\eta)$, respectively for different values of first order slip parameters a_1, a_2 when $s = 2$, $\lambda = -2.2$ and $b_1, b_2 = 0$. Further, the effects of the second order slip parameter b_1, b_2 on the velocity profiles $f'(\eta)$ and $g'(\eta)$ when $s = 2$, $\lambda = -2.2$ and $a_1, a_2 = 0$ are shown in Figs 9 and 10, respectively. From these figures, it is seen that for the given suction and stretching/shrinking parameters, the boundary layer thickness for both solution branches becomes smaller with the increase of the slip parameters. Increasing slip allows more fluid to flow through the surface, thus reducing the boundary layer thickness. All profiles displayed in Figs. 7-12 satisfy the far field boundary conditions (2.11) asymptotically, thus supporting the validity of the dual solutions obtained in this study.

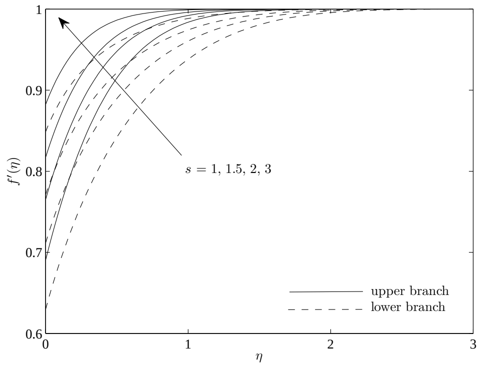

FIGURE 11. Velocity profiles $f'(\eta)$ for different values of s when $\lambda = -2.2$, $a_1 = 1.5$, $b_1 = -1.5$, $a_2 = 1$ and $b_2 = -1$

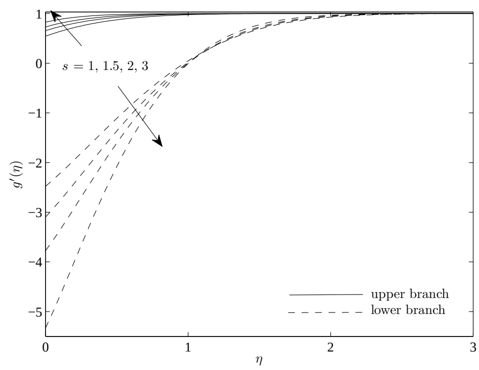

FIGURE 12. Velocity profiles $g'(\eta)$ for different values of s when $\lambda = -2.2$, $a_1 = 1.5$, $b_1 = -1.5$, $a_2 = 1$ and $b_2 = -1$

4. Conclusion

The problem of steady three-dimensional stagnation-point flow of a viscous and incompressible fluid past a permeable stretching/shrinking sheet with second order slip flow model has been studied numerically. This problem was solved by using the `bvp4c` function from MATLAB. The effects of the suction parameter s, first order slip parameters a_1, a_2 and second order slip parameters b_1, b_2 have been analyzed and presented. Multiple (dual) solutions are found for a certain range of the suction and stretching/shrinking parameters. The suction parameter widens the range of stretching/shrinking parameter for which similarity solutions exist. The values of the reduced skin friction coefficients are found to increase with the increase of suction and stretching/shrinking parameters, while decrease with the increase of slip parameters.

Acknowledgment

This work was supported by research grant (GP-IPM/2018/9619000) from Universiti Putra Malaysia, Malaysia.

References

[1] K. Hiemenz: *Die Grenzschicht an einem in den gleichformingen Flussigkeitsstrom eingetauchten graden Kreiszylinder*, Dinglers Polytech J **326** (1911), 321–324.
[2] F. Homann: *Der Einfluss grosser Zahigkeit bei der Stromung um den Zylinder und um den Kugel*, Z. Angew. Math. Mech. **16** (1936), 153–164.
[3] P. Libby: *Wall shear at a three dimensional stagnation point with a moving wall*, AIAA J. **12** (1974), 408–409.
[4] P. Weidman, M. Sprague: *Flows induced by a plate moving normal to stagnation-point flow*, Acta Mech. **219** (2011), 219–229.
[5] N. S. Khashi'ie, N. M. Arifin, I. Pop, N. S. Wahid: *Effect of suction on the stagnation point flow of hybrid nanofluid toward a permeable and vertical riga plate*, Heat Transfer **50**(2) (2021), 1895–1910.
[6] L. Wu: *A slip model for rarefied gas flows at arbitrary Knudsen number*, Appl Phys Lett **93** (2008), art.no. 253103.
[7] T. Fang, S. Yao, J. Zhang, A. Aziz: *Viscous flow over a shrinking sheet with a second order slip flow model*, Commun. Nonlinear Sci. Numer. Simul. **15**(7) (2010), 1831–1842.

[8] M. NANDEPPANAVAR, K. VAJRAVELUB, M. SUBHAS ABEL, M. SIDDALINGAPPAA: *Second order slip flow and heat transfer over a stretching sheet with non-linear Navier boundary condition*, Int. J. Therm. Sci. **58** (2012), 143–150.

[9] S. SOID, J. MERKIN, A. ISHAK, I. POP: *Axisymmetric stagnation-point flow and heat transfer due to a stretching/shrinking vertical plate with surface second-order velocity slip*, Meccanica (2016) 1–13.

[10] I. WAINI, A. ISHAK, I. POP: *Melting heat transfer of a hybrid nanofluid flow towards a stagnation point region with second-order slip*, Proceedings of the Institution of Mechanical Engineers, Part E: Journal of Process Mechanical Engineering **235**(2) (2021), 405–415.

CENTRE OF FOUNDATION STUDIES FOR AGRICULTURAL SCIENCE,
UNIVERSITI PUTRA MALAYSIA,
43400 UPM SERDANG, SELANGOR,
MALAYSIA.
Email address: ezadhafidz@upm.edu.my

SCHOOL OF MATHEMATICAL SCIENCES,
FACULTY OF SCIENCE AND TECHNOLOGY,
UNIVERSITI KEBANGSAAN MALAYSIA,
43600 UKM BANGI, SELANGOR, MALAYSIA.
Email address: rmn@ukm.edu.my

DEPARTMENT OF MATHEMATICS
UNIVERSITI PUTRA MALAYSIA,
43400 UPM SERDANG, SELANGOR,
MALAYSIA.
Email address: norihana@upm.edu.my

DEPARTMENT OF MATHEMATICS,
BABES-BOLYAI UNIVERSITY,
400084 CLUJ-NAPOCA,
ROMANIA.
Email address: popm.ioan@yahoo.co.uk